

Influence of the Stellar Population on Type Ia Supernovae: Consequences for the Determination of Ω

P. Höflich¹, K. Nomoto², H. Umeda², J.C. Wheeler¹

1. *Department of Astronomy, University of Texas, Austin, TX 078712, USA*

2. *Department of Astronomy & Research Center for the Early Universe, University of Tokyo, Tokyo 113-0033, Japan*

ABSTRACT

The influence of the metallicity at the main sequence on the chemical structure of the exploding white dwarf, the nucleosynthesis during the explosion and the light curves of an individual Type Ia supernovae have been studied. Detailed calculations of the stellar evolution, the explosion, and light curves of delayed detonation models are presented.

Detailed stellar evolution calculations with a main sequence mass M_{MS} of $7 M_{\odot}$ have been performed to test the influence of the metallicity Z on the structure of the progenitor. A change of Z influences the central helium burning and, consequently, the size of the C/O core which becomes a C/O white dwarf and its C/O ratio. Subsequently, the white dwarf may grow to the Chandrasekhar mass and explode as a Type Ia supernovae. Consequently, the C/O structure of the exploding white dwarf depends on Z . Since C and O are the fuel for the thermonuclear explosion, Z indirectly changes the energetics of the explosion.

In our example, changing Z from Pop I to Pop II causes a change in the zero point of the maximum brightness/decline relation by about 0.1^m and a change in the rise time by about 1 day. Combined with previous studies, the offset in the maximum brightness/decline $\Delta M \approx \Delta t$ where Δt is the change of the rise time in days.

Systematic effects of the size discussed here may well make the results from the SNe Ia searches consistent with an Universe with $\Omega_M = 0.2$ and $\Omega_{\Lambda} = 0$ but hardly will change the conclusion that we live in a universe with low Ω_M . Variations of the expected size may prove to be critical if, in the future, SNe Ia are used to measure large scale scalar-fields because Z may show large local variations. Evolutionary effects will not change substantially the counting rates for SNe Ia even at very large red-shifts.

Evolutionary effects may be of the same order as the brightness changes related to cosmological parameters, but we have shown ways, how the effects of evolution can be detected.

Subject headings: Supernovae: general – nucleosynthesis – radiation transfer – large-scale structure of universe

1. Introduction

Two of the important new developments in observational supernova research in the last few years were to establish the long-suspected correlation between the peak brightness of SNe Ia and their rate of decline by means of modern CCD photometry (Phillips 1993) and the exact distance calibrations provided by a HST project (e.g. Saha et al. 1997). This allowed an empirical determination of H_o with unprecedented accuracy (Hamuy et al. 1996, Riess et al. 1995). Independent from these calibrations and empirical relations, H_o has been determined by comparison of detailed theoretical models for light curves and spectra with observations (Müller & Höflich 1994, Höflich & Khokhlov 1996, Nugent et al. 1996). All determinations of the Hubble constant are in good agreement with one another. More recently, the routine successful detection of supernovae at large redshifts, z (e.g. Perlmutter et al. 1999, Riess et al. 1998), has provided an exciting new tool to probe cosmology. This work has provided results that are consistent with a low matter density in the Universe and, most intriguing of all, yielded hints for a positive cosmological constant. These results are based on empirical brightness-decline relations which are calibrated locally. This leaves systematic effects as the main source of concern. In this respect, theoretical models provide a critical tool to estimate the possible size of evolutionary effects, how these effects can be recognized and how one may be able to correct for them.

The primary scenario for SNe Ia consists of massive carbon-oxygen white dwarfs (WDs) in a close binary system which accrete through Roche-lobe overflow from low mass companion star when it evolving away from the main sequence or during its red giant phase (Nomoto & Sugimoto 1977). The WD is the final evolution of stars with a main sequence masses smaller than $\approx 8 M_\odot$ which has lost his H/He rich envelope with the C/O core of $\approx 0.5...1.2M_\odot$. If accretion is sufficient large (i.e. $\geq 2...4 \cdot 10^{-8} M_\odot/yr$), the accreted H burns to He and, subsequently, to C/O on the surface of the WD and the mass of the WD grows close to the Chandrasekhar mass M_{Ch} . The corresponding time scales for growing to M_{Ch} are $\leq 5 \times 10^7 yrs$. In these accretion models, the explosion is triggered by compressional heating close to the center.

Höflich, Khokhlov & Wheeler (1995) showed that models based on Chandrasekhar mass carbon-oxygen

white dwarfs can account for subluminous as well as “normally bright” SNe Ia. The basic paradigm of these models is that thermonuclear burning begins as a subsonic, turbulent deflagration and then makes a transition to a supersonic, shock-driven detonation (Khokhlov 1991ab, Yamaoka et al. 1992, Woosley & Weaver 1994). These models are generally known as delayed detonation models. In this class of models the amount of nickel produced is a function of the density at which the transition is made from deflagration to detonation, the central density, metallicity and the chemical structure of the initial WD (Höflich et al. 1995, Höflich & Khokhlov 1996, Höflich, Wheeler & Thielemann 1998, HWT98 hereafter). The radioactive decay of the variable nickel mass is the dominant factor which gives a range in maximum brightness and ^{56}Ni is the most important factor which governs the light curve shape. The models with less nickel are not only dimmer, but are cooler and have lower opacity, giving them redder, more steeply declining light curves. A given amount of nickel can be produced by different combinations of the model parameters and, from the models, we expect a spread around the mean maximum brightness-decline relation of ≈ 0.3 to 0.5^m . A similar spread of $\approx \pm 0.4^m$ ($\sigma \approx 0.18^m$ in B) in the local, observed relation between maximum brightness and decline (Hamuy et al. 1996) may also suggest that there are additional parameters needed in the empirical relations. Note that new observations and recalibrations of the old observations indicate a somewhat tighter relation ($\approx 0.12^m$, Jha et al. 1999; Kirshner et al., 1999). From the current status of theoretical models, this very narrow spread cannot be understood, but it cannot be ruled out either. Both reanalysis of new light curves and theoretical investigation of the coupling between the “free” parameters may help to answer this puzzle. Note that this also implies that observable spreads in relations, e.g. between rise time and decline time, cannot be expected to change along the path given by the change of a particular free model parameter.

There are some hints that SN Ia have undergone evolutionary effects. Branch et al. (1996) have shown that the mean peak brightness is dimmer in ellipticals than in spiral galaxies. Wang, Höflich & Wheeler (1997) found that the peak brightness in the outer region of spirals is similar to those found in ellipticals, but that in the central region both intrinsically brighter and dimmer SNe Ia occur. This implies that the underlying progenitor populations are more

inhomogeneous in the inner parts of spiral galaxies which contain both young and old progenitors. Systematic effects that must be taken into account in the use of SNe Ia to determine cosmological parameters include technical problems, changes of the environment with time, changes in the statistical properties of the SNe Ia, and changes in the physical properties of SNe Ia.

In a previous paper (HWT98), the effect of the change of the initial metallicity and the C/O ratio on light curves and spectra was studied by changing both the C/O ratio and the metallicity independently. It was found that a reduction in the C/O ratio mainly effects the energetics of the explosion. The ^{56}Ni production are reduced and the Si-rich layers are more confined in velocity space for smaller C/O. Moreover, the brightness to decline ratio can change causing a shift in the zero point of the maximum brightness decline relation of $\approx 0.3^m$. Such a shift can be detected by a corresponding change in the rise time by about 3 days. The influence of the metallicity is especially important with respect to the ^{54}Fe production in the outer layers which govern the spectra in the UV and blue; however, the influence on the resulting rest frame visual and blue light curves is found to be small. A separation of the effects of Z and the C/O ratio in the WD is justified because the metallicity is inherited from the ISM when it is formed and the C and O are produced during the progenitor evolution. To first order, the C/O ratio depends on the zero age main sequence mass. Consequently, a systematic shift in the maximum brightness/decline relation can be produced by a change with redshift of the typical progenitor mass. This effect is expected as the mean life time becomes shorter if we are looking back closer to the star forming period.

To second order, however, one must take into account that the metallicity also influences the stellar evolution during central helium burning. The possible consequences for evolutionary effects in SNIa and the influence of $^{12}\text{C}(\alpha, \gamma)$ -rate as has been pointed out recently by various groups (Nomoto et al. 1997; Dominguez et al. 1999; Höflich et al. 1999; Umeda et al. 1999a). Thus, besides changing the C/O ratio as a consequence of the change in the typical progenitor mass, the effects of metallicity discussed above may also apply to individual SNe Ia of a given main sequence mass.

In this paper we study the latter effect: the influence of the metallicity on an individual supernova

with respect to the nucleosynthesis and light curves. We investigate the size of the shift of the zero point in the brightness/decline relation and the consequences for the use of SNIe Ia for cosmology. We address the issue how to distinguish the effect of a change in the "typical" progenitor from the effect of the metallicity on the chemical structure of an individual progenitor.

2. Brief Description of the Numerical Methods

2.1. Stellar Evolution

The stellar evolution has been calculated using the code of Nomoto's group up to the end of the helium burning. These calculations have already been published and discussed in detail by Umeda et al. (1999a). Subsequently, the evolution of the C/O core is calculated by accreting H/He rich material at a given constant accretion rate on the core by solving the standard equations for stellar evolution using a Henye scheme. Nomoto's equation of state is used (Nomoto et al. 1982). Crystallization is neglected. For the energy transport, conduction (Itoh et al. 1983), convection in the mixing length theory, and radiation are taken into account. Radiative opacities for free-free and bound-free transitions are treated in Kramer's approximation and by free electrons. A nuclear network of 35 species up to ^{24}Mg is taken into account. Here, we do not include convective mixing at the onset of ignition of the deflagration front at the center. Depending on the description, the entire WD may mixed be mixed (Nomoto, Sugimoto & Neo 1976, Höflich et al. 1998). Although this may change the central carbon concentration at the center, the energetics of the explosions will not change.

2.2. Hydrodynamics

The explosions are calculated using a one-dimensional radiation-hydro code, including nuclear networks (Höflich & Khokhlov 1996 and references therein). This code solves the hydrodynamical equations explicitly by the piecewise parabolic method (Collela & Woodward 1984) and includes the solution of the frequency averaged radiation transport implicitly via moment equations, expansion opacities (see below), and a detailed equation of state. Nuclear burning is taken into account using a network which has been tested in many explosive environments (see Thielemann et al. 1996 and references therein).

2.3. Light Curves

Based on the explosion models, the subsequent expansion and bolometric as well as broad band light curves are calculated using a scheme recently developed, tested and widely applied to SN Ia (e.g. HWT98 and references therein). The code used in this phase is similar to that described above, but nuclear burning is neglected and γ ray transport is included via a Monte Carlo scheme. In order to allow for a more consistent treatment of scattering, we solve both the (two lowest) time-dependent, frequency averaged radiation moment equations for the radiation energy and the radiation flux, and a total energy equation. At each time step, we then use $T(r)$ to determine the Eddington factors and mean opacities by solving the frequency-dependent radiation transport equation in the comoving frame and integrate to obtain the frequency-averaged quantities. About one thousand frequencies (in one hundred frequency groups) and about five hundred depth points are used. The averaged opacities are calculated under the assumption of local thermodynamical equilibrium. Both the monochromatic and mean opacities are calculated using the Sobolev approximation (Sobolev 1957). The scattering, photon redistribution and thermalization terms used in the light curve opacity calculation are calibrated with NLTE calculations using the formalism of the equivalent-two-level approach (Höfllich 1995).

3. Results

The initial mass of the C/O WD is given by the results of stellar evolution. Its mass depends on M_{MS} of the progenitor and Z . At the time of the explosion, the WD masses are close to the Chandrasekhar limit. The WD has grown by accretion of H/He and subsequent burning. In the accreted layers, the C/O- ratio is close to 1.

Here, we study the size of the metallicity effect using as an example a $7 M_{\odot}$ with Population I ($Z=0.02$) and II ($Z=0.004$) compositions (Fig. 1). We assume that the relative abundance within the metals is solar. In reality, the [O/Fe] changes with the metallicity and we may separate between Z_{CNO} and Z_{Fe} . The former governs the CNO cycle including the production of neon which determines the proton to nucleon ratio and, consequently, the abundances of the iron group elements produced during the thermonuclear explosion. This will effect the spectra at maximum light

(see HWT98) but hardly the size of the C/O ratio which is the main subject of this letter. It is the iron abundance that governs the opacity and changes the core size. The metallicity Z of heavy elements, e.g. Fe, mainly effects the convection during stellar Helium burning and, consequently, the size of the C/O core and the central C/O ratio. We note that the exact size of the effect and its sign depends on the mass of the progenitor on the zero age main sequence, and Z . Even for a given mass, the changes are not monotonic, but may change sign from Pop I to Pop II to Pop III (Umeda et al. 1999a, Dominguez et al. 1999). In addition, the variation depends sensitively on the assumed physics such as the $^{12}C(\alpha, \gamma)^{16}O$ -rate (e.g. Straniero et al. 1997). Our example can serve as a guide to estimate the size of this effect, but will not give all possible variations.

At the time of the explosion, the central density has been fixed at $\rho_c = 2.4E9g/cm^{-3}$. The ratio α of the deflagration velocity to the sound speed has been set to 0.02 and the transition density ρ_{tr} at which the deflagration is assumed to turn into a detonation is $2.4 \cdot 10^7 g cm^{-3}$. The parameters are close to those which reproduce both the spectra and light curves reasonably well (Nomoto et al. 1984; Höfllich 1995; Höfllich & Khokhlov 1996).

The total abundances of the most important elements are given for the model in Table 1. Fig. 2 gives the density and velocity versus mass for the models with the Pop I and Pop II metallicity, respectively. Fig. 3 gives the composition profiles of the major elements for the same models. The overall density and velocity structures are insensitive to changes in the underlying model. Qualitatively, the final burning products can be understood by the relation between hydrodynamic and the nuclear time scales. Since most of the energy is released by the explosive burning of carbon and oxygen, the energy production per gram depends on the initial chemical composition of the WD, i.e. the C/O ratio. The nuclear time scales are determined by the peak temperature during burning, which depends on the energy release per volume because the energy density is radiation dominated. Since the energy release per gram is fixed, the peak temperature is given by the composition and the local density. Thus, the latter variables are the dominant factors that determine the final composition of a zone. After accretion on the initial core, the total mass ratio of M_C/M_O is 0.75 and 0.61 for the models with Pop I and II, respectively. The total

Table 1: Total abundances of the delayed detonation model for high and low metallicity

Population	He	C	O	Mg	Si	S	Ca	Fe
I	2.0E-04	2.0E-02	6.8E-02	1.4E-02	2.2E-01	1.3E-01	2.2E-02	4.5E-01
II	5.5E-05	2.2E-02	7.2E-02	1.5E-02	2.4E-01	1.4E-01	2.4E-02	4.1E-01

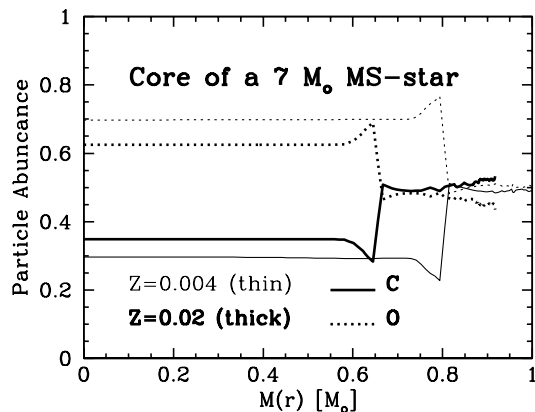


Fig. 1.— Chemical profile of the C/O core of a star with the main sequence mass of $7M_{\odot}$ after central Helium burning.

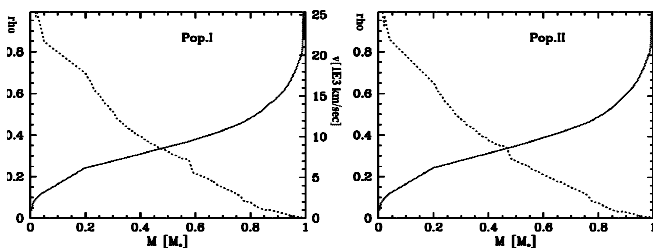


Fig. 2.— Density and velocity as a function of mass for the delayed detonation model originating from progenitors with PopI and Pop II composition.

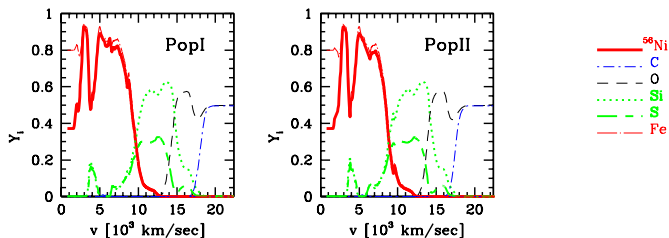


Fig. 3.— Same as Fig. 2, but abundances as a function of the final expansion velocity. Both the initial ^{56}Ni and the final Fe profiles are shown.

nuclear energy release depends on the total C/O ratio, but the structure of the WD is unaffected by a change in metallicity (HWT98). Therefore, the final kinetic energy is reduced from $1.41 \times 10^{51} \text{erg}$ for $Z=0.02$ to $1.37 \times 10^{51} \text{erg}$ for $Z=0.004$. The nuclear energy production during burning decreases with the C/O ratio at the burning front and, consequently, the transition density is reached later in time. The resulting larger pre-expansion of the outer layers reduces the ^{56}Ni production from 0.56 to $0.51 M_{\odot}$ for the Pop I and II model, respectively, and the transition regions between complete and incomplete C and O burning changes by about 500 km s^{-1} .

As discussed in HWT98, a change of the metallicity changes also the abundances of trace elements such as ^{54}Fe (Fig. 4). The reason is that the metallicity mainly affects the initial CNO abundances of a star. These are converted during the pre-explosion stellar evolution to ^{14}N in H-burning and via $^{14}\text{N}(\alpha, \gamma)^{18}\text{F}(\beta^+)^{18}\text{O}(\alpha, \gamma)^{22}\text{Ne}$ to nuclei with $N=Z+2$ in He-burning. The result is that increasing metallicity yields a smaller proton to nucleon ratio, Y_e , throughout the pre-explosive WD (Thielemann et al. 1997, HWT98). Higher metallicity and smaller Y_e lead to the production of more neutron-rich Fe group nuclei and less ^{56}Ni . For lower metallicity and thus higher Y_e , some additional ^{56}Ni is produced at the expense of ^{54}Fe and ^{58}Ni (Thielemann, Nomoto & Yokoi, 1986). We note that these layers with $v \geq 12,000 \text{ km s}^{-1}$ dominate the spectra around maximum light and lines of the iron group, but have little influence on the light curves.

Light curves provide a valuable tool to probe the underlying explosion models, namely the absolute amount of ^{56}Ni and its distribution. Broad-band light curves are shown in Fig. 5. As expected from the last section, the main effect on the light curves is caused by the change in the explosion energy and the ^{56}Ni production. The change in the maximum brightness remains small ($M_V(\text{PopI}) - M_V(\text{PopII}) = -0.03^m$) and the rise times are different by about 1 day ($t_B(\text{PopI}) = 16.4d$ vs. $t_B(\text{PopII}) = 17.6d$). The smaller expansion due to the smaller E_{kin} causes a reduced geometrical dilution of the matter and a re-

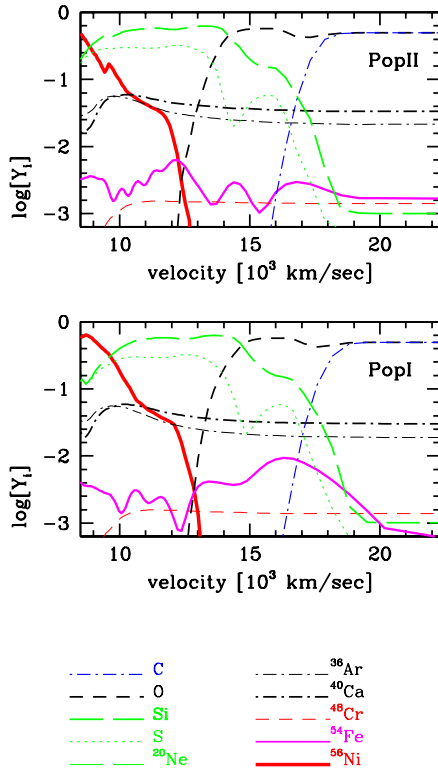


Fig. 4.— Same as Fig. 2, but abundances of different isotopes as a function of the expansion velocity for layers with partial burning.

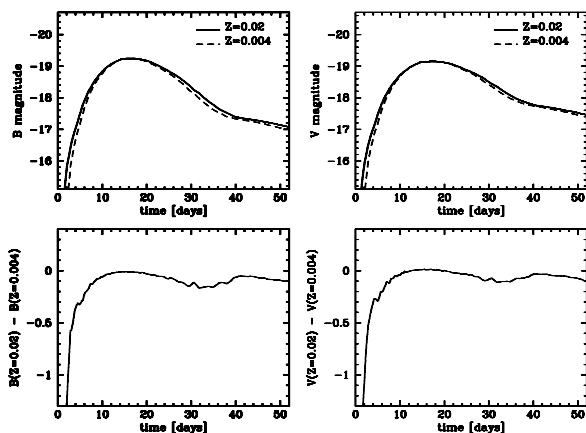


Fig. 5.— Comparison of light curves in B and V of the delayed detonation models with metallicities corresponding to Pop.I and Pop. II.

duction of the expansion work at a given time. Consequently, for Pop II, the rise time to maximum light is slower by about 1 days and the maximum brightness is only slightly smaller despite the 10 % reduced production of ^{56}Ni because, in the latter case, more of the stored energy goes into the radiation rather than kinetic energy, and energy can be stored for a longer time. The most significant effect is a steeper decline ratio and a reduced ^{56}Ni production for the Pop II-model. This translates into a systematic offset of $\approx 0.1^m$ in the maximum brightness decline ratio somewhat depending on the slope derive from the data (Phillips 1992, Hamuy et al. 1996). Using either the stretching method or the LCS-method gives similar offsets.

4. Conclusions

The influence of the metallicity at the main sequence on the chemical structure of the exploding white dwarf, the nucleosynthesis during the explosion, and the light curves of individual Type Ia supernovae have been studied using the example of delayed detonation models¹. Model parameters are used for which the theoretical optical and infrared light curves and of the spectral evolution resembles those of a normal bright SNe Ia. Note that we did not tune the parameter that the specific example resembles a particular supernova or a specific normalization such as a stretch factor $s=1$.

A change of the metallicity influences the central helium burning and, consequently, the size of the C/O core which becomes a C/O WD and its C/O ratio. The WD may grow to the Chandrasekhar mass and explode as a Type Ia supernovae. Consequently, the metallicity changes the C/O structure of the exploding white dwarf. As C and O are the fuel

¹Addendum: In this paper, we consider the dependence of the brightness-decline rate relation and changes in the rise times on X_C for given model parameters. We assume that the C/O ratio has little effect on the nuclear burning. In contrast, Umeda et al. (1999b) considered the influence of X_C on the transition density and, thus, on the production of radioactive Ni. Fully consistent with previous papers (Höflich 1995, Höflich, Khokhlov & Wheeler 1995), they find that the Ni production declines with the transition density between deflagration and detonation. The absolute brightness declines accordingly (HK96). Umeda et al. (1999) do not consider the effect of X_C on the brightness-decline rate relation or the rise times. Instead, for an assumed relation between transition density and C/O ratio, they discuss the implications on the typical brightness as a function of red-shift based on their study for progenitor evolution.

for the thermonuclear explosion, the metallicity indirectly changes the energetics of the explosion. In addition, the metallicity alters the isotopic composition of the outer layers of the ejecta that have undergone explosive O burning. Especially important is the increase of the ^{54}Fe production with metallicity which alters the spectra near maximum light (HWT98).

As the C/O ratio of the WD is decreased, the explosion energy and the ^{56}Ni production are reduced. Changing the initial metallicity from Pop I to Pop II changes the rise times by about 1 day, and causes a small decrease in luminosity at maximum light, a faster post-maximum decline and a larger ratio between maximum light and ^{56}Ni tail by about 0.1^m . This effect is equivalent to a change from a one-parameter maximum brightness/decline relation which is widely used to determine the cosmological parameters Ω_M and Ω_Λ . In our example, the calibration of the $\Delta M(dM_{15})$ relation is changed by about 0.1^m . From previous studies of the stellar evolution for different masses and metallicities (Umeda et al. 1999a, Dominguez et al. 1999), the influence of Z on the C/O ratio is comparable to our example, but the sign may change depending on details of the nuclear cross sections and the treatment of convection, and the mass and metallicity range. In our example, the systematic change in the progenitor metallicity from Pop I to Pop II translates into a shift of the confidence regions in the $\Omega_M - \Omega_\Lambda$ plane based on high-z SNeI a (Riess et al. 1998; Perlmutter et al. 1999) by about 0.15 and 0.7 along the small and large axes of the error ellipsoids. However, a change of typical progenitor from Pop I to II is unlikely for the redshifts currently used to determine Ω_M and Ω_Λ because we see a large variation of metallicities in our galaxy (Edvardsson et al., 1993ab).

Even strong variations in the metallicity will hardly produce selection effects with respect to the counting rates for SNe Ia at large red-shifts. Variations of the expected size are critical if, in future, SNe Ia may be used to measure large scale scalar-fields because the metallicity may show large local variations during the early phases when individual SNe explosions govern the metallicity.

A change of the C/O ratio reveals itself mainly by the change in the ratio between rise time and decline. This change may be caused either by a change of Z or, alternatively, by a change of the main sequence mass of the progenitor. When using statistical methods to determine cosmological parameters, both a change in

the distribution of progenitor masses and the metallicity of the sample may cause systematic evolutionary effects. Fortunately, it does not matter whether a change of C/O is due to a change in the metallicity or the typical mass of the progenitors. In both cases, we find that $\Delta M \approx \Delta t_{rise}$ where ΔM is the offset in the maximum brightness/decline relation in magnitudes and Δt is measured in days (compare HWT98).

The effect of progenitor mass and metallicity can be untangled by simultaneous analysis of both spectra and light-curves. In principle, this allows a method to get a handle on the progenitor mass. With the current level of modeling such analysis is restricted to differential comparisons between individual supernovae.

After submission of this paper, a comparison of rise times between local and distant supernovae has been submitted (Riess et al. 1999). They find a difference in the rise times between the local and the distant sample of 2.5 ± 0.4 days if all observed supernovae are normalized to the stretch factor s of 1. This result is based on a preliminary analysis of the high redshift data by Goldhaber (1998). It may also be noted that both the local and the distant sample show a spread of ± 1 day in the rise time/decline relation without overlap which is hard to understand. However, if confirmed and in light of our analysis, this would imply a systematic offset $\approx 0.25^m$ in the brightness decline relation. A change of this order would not alter the basic conclusion of the high z searches that we live in a low Ω universe but, then, a low Ω universe with $\Omega_M = 0.2$ and $\Omega_\Lambda = 0$ may be consistent with SN data as well.

The following trend for the theoretical models is worth noting: For realistic cores, the both the mean M_C/M_O and the M_C/M_O in the central regions of the WD tend to be smaller than the canonical value of 1 used in all calculations prior to 1998 (e.g. Nomoto et al. 1984, Woosley & Weaver 1994, Höflich & Khokhlov 1996). Consequently, as a general trend, the rise times are about 1-4 days slower compared to models published before 1998.

ACKNOWLEDGMENTS

We thank the referee for useful discussions and helpful comments. This research was supported in part by NASA Grant LSTA-98-022, NASA Grant NAG5-3930, NSF Grant AST-9528110, and the grant-in-Aid for COE Scientific Research (07CE2002) of the

Ministry of Education, Science and Culture in Japan. The calculations for the explosion and light curves were done on a cluster of workstations financed by the John W. Cox-Fund of the Department of Astronomy at the University of Texas.

REFERENCES

- Branch D., et al. 1998, Phys. Rep., in press
- Collela P., Woodward P.R. 1984, J.Comp.Phys., 54, 174
- Dominguez I. Höflich P., Straniero O., Wheeler J.C. 1999, in: Nuclei in the Cosmos V, ed. N. Pranzos, (Paris: Editions Frontiers)
- Edvardsson B., Andersen J., Gustafsson B., Lambert D.L., Nissen P.E., Tomkin J. 1993a, A&A, 275, 101
- Edvardsson B., Andersen J., Gustafsson B., Lambert D.L., Nissen P.E., Tomkin J. 1993b, A&AS. 102, 603
- Goldhaber G. 1998, BAAS, 193, 4713 Tomkin J. 1993b, A&AS. 102, 603
- Hamuy M. et al. 1996, AJ, 112, 2438
- Höflich P. 1995, ApJ, 443, 89
- Höflich P., Khokhlov A., Wheeler J.C. 1995, ApJ, 444, 831
- Höflich P., Khokhlov A. 1996, ApJ, 457, 500
- Höflich P., Khokhlov A., Wheeler J.C., Phillips M., Suntzeff N., Hamuy M., 1996, ApJ, 472, 81
- Höflich P., Wheeler J.C., Thielemann F.K 1998, ApJ, 495, 617 (HWT98)
- Höflich P., Dominguez I., Thielemann F.K., Wheeler J.C. 1998, in: The Next Generation Space Telescope, ESA-SP-429, ESTEC, Noordwijk, The Netherlands, p. 243
- Itoh N., Mitake S., Iyetomi H., Ichimaru S. 1983, ApJ 273, 774
- Jha S. et al. 1999, ApJS, submitted and astro-ph/9906220
- Khokhlov A. 1991ab, A&A, 245, 114 & L25
- Kirshner R.P., 1999, in: SNe Ia and Cosmology, Kluwer Press, eds. J.Niemeyer et al., Chicago, in press
- Müller E., Höflich P. 1994, A&A, 281, 51
- Nomoto K., Sugimoto S., Neo S. 1976, ApSS, 39, L37
- Nomoto K., Sugimoto D. 1977, PASJ, 29, 765
- Nomoto K., 1982, ApJ, 253, 798
- Nomoto K., Thielemann F.-K., Yokoi K. 1984, ApJ, 286, 644
- Nugent P., et al. 1996, Phys. Rev. Let., 75, 394 & 1974E
- Phillips M.M. et al. 1987, PASP, 90, 592
- Phillips M. M., 1993, ApJ, 413, L108
- Perlmutter S. et al. 1999, ApJ, in press and astro-ph/9812473
- Riess A.G., Press W.H., Kirshner R.P., 1995, ApJ, 438, L17
- Riess A. et al. 1998, AJ 116, 1009
- Riess A., Filippenko A., Weidong L., Schmidt B. 1999, AJ, submitted & astro-ph/9907038
- Saha A. et al. 1997, ApJ 486, 1
- Sobolev, V.V., 1957, Sov. Astron., 1, 297
- Thielemann F.K., Nomoto K., Hashimoto M. 1996, ApJ, 460, 408
- Thielemann F.K., Nomoto K., Yokoi K. 1986, A&A, 158, 17
- Umeda H., Nomoto K., Yamaoka H., Wanao S. 1999a, ApJ, 513, 861
- Umeda, H., Nomoto, K., Kobayashi, C., Hachisu, I., Kato, M. 1999b, ApJ 522, L43
- Wang L., Höflich P., Wheeler, J.C. 1997, ApJ, 487, L29
- Woosley S. E. & Weaver T. A. 1994, Proc. of Les Houches Session LIV, eds. Bludman et al., North-Holland, 63
- Yamaoka H., Nomoto K., Shigeyama T., Thielemann F., 1992, ApJ, 393, 55

This 2-column preprint was prepared with the AAS L^AT_EX macros v4.0.